ACS APPLIED MATERIALS & INTERFACES

Letter

www.acsami.org

Increased Graphitization in Electrospun Single Suspended Carbon Nanowires Integrated with Carbon-MEMS and Carbon-NEMS Platforms

Swati Sharma,[†] Ashutosh Sharma,*[,‡] Yoon-Kyoung Cho,[†] and Marc Madou*[,§]

[†]School of Nano-Bioscience and Chemical Engineering, Ulsan National Institute of Science and Technology, Ulsan 689-798, South Korea

[‡]Department of Chemical Engineering, Indian Institute of Technology, Kanpur 208016, U.P., India

[§]Department of Mechanical & Aerospace Engineering, University of California, Irvine, California, United States 92697-3975

ABSTRACT: Single suspended carbon nanowires (CNWs) integrated on carbon-MEMS (CMEMS) structures are fabricated by electrospinning of SU-8 photoresist followed by pyrolysis. These monolithic CNW-CMEMS structures enable fabrication of very high aspect ratio CNWs of predefined length. The CNWs thus fabricated display core–shell structures having a graphitic shell with a glassy carbon core. The electrical conductivity of these CNWs is increased by about 100% compared to glassy carbon as a result of enhanced graphitization. We suggest some tunable fabrication and pyrolysis parameters that may improve graphitization in the resulting CNWs, making them a good replacement for several carbon nanostructure-based devices.

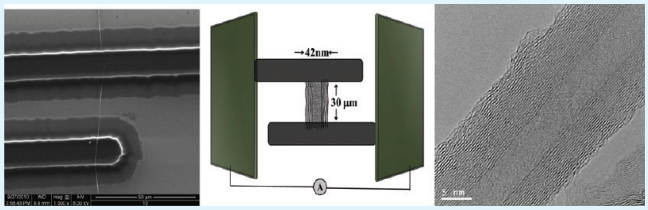

KEYWORDS: *carbon nanowire, carbon-MEMS, photolithography, electrospinning, graphitization*

In the past two decades, carbon has received much attention as a material to possibly compete with silicon for the construction of miniaturized devices such as ICs and micro- and nano-electromechanical systems (MEMS and NEMS).[1−6] Carbon occupies a very special place both in nature and technology because of the widely different structures and properties of its various forms.[7−9] Glassy carbon electrodes offer a wide electrochemical stability window, low-background currents, and low cost.[1,10,11] Graphitic and hard carbons in battery applications are well suited because of their reversible Li intercalation/deintercalation capacity.[12] Further, carbon nanotubes (CNTs), graphene and carbons with higher graphitic content are of tremendous current interest in both fundamental research and for nanoelectronics applications.[13−17] Here we introduce CMEMS and CNEMS platforms as a means of fabrication, positioning, and integration of single suspended carbon nanowires (CNWs) with good and reproducible ohmic contacts.

The main challenges in the fabrication of single CNW or CNT based devices are their positioning and integration with the underlying platforms and in establishing a reliable ohmic contact. In most cases, the nanowires are first synthesized and isolated, and then carefully nanopositioned and integrated, e.g., by placing on a flat substrate followed by deposition of metal electrodes over their ends.[18−20] These are cumbersome and low-throughput techniques that are not suitable for manufacturing of solid-state devices. Also, the contact resistance varies from sample to sample and the contact with the substrate can interfere with the properties of the nanowires. Here we present a simple and scalable fabrication technique for positioning and integration of suspended CNWs with good ohmic contacts. This technique enables fabrication of single, well separated CNWs that are pulled in tension on the CMEMS, and isolation of a single CNW from bulk is not required. This is achieved by electrospining of polymer nanowires on an underlying polymeric MEMS platform fixed on a rotating drum, followed by pyrolysis of the suspended nanowires plus their platform to produce a carbon monolith. The current technique enables the fabrication of CNWs of predefined lengths at preselected locations of interest, which are difficult to achieve with other methods. Further, we show that this method produces CNWs of higher graphitic content and electrical conductivity than glassy carbon and the extent of graphitization can be tuned by controlling the fabrication parameters.

It is known that in the pyrolysis process, polymer precursors retain their original morphology and chain configurations.[21] Therefore, it is extremely important to first obtain polymer nanofibers with maximized chain disentanglements in order to get more graphitic resulting CNWs. Tangled polymer chains yield glassy carbons that cannot be reverted back to graphite even at very high temperatures,[21−23] because it is not possible to unwind the polymer chains once converted to carbon.

The parameters that may influence the extent of disentanglement of polymer chains, and in turn, the extent of

Received: October 18, 2011
Accepted: January 3, 2012
Published: January 3, 2012

   dx.doi.org/10.1021/am2014376 | *ACS Appl. Mater. Interfaces* 2012, 4, 34–39

graphitization in the CNWs include (1) nature of the precursor polymer (e.g., its chemical composition and viscoelasticity),[24] (2) thickness of the polymer wires,[25] (3) carbonization temperature,[22] (4) alignment of polymer molecules by the flow pattern of the polymer and nozzle size,[25,26] (5) mechanical pulling of the polymer molecules,[27,28] (6) alignment of polymers chains caused by high electric fields,[29] (7) catalysts in the precursor polymer,[30] and (8) templating.[31,32]

In addition to these reported parameters, we believe that mechanical pulling of the suspended polymer nanofiber is also affected in other ways. For example, during the carbonization process itself, say when employing SU-8 walls to hold the fiber, the shrinkage of these walls to almost one forth their original size (horizontally) gives an extra pull to the suspended fibers. We chose to work further with SU-8 derived nanowires because it is the material of choice for MEMS fabrication, allowing a wider range of MEMS structures with tunable designs due to its compatibility with conventional photolithography. Further, SU-8 fibers should display better adhesion and integration with SU-8 MEMS structures because of the same glass transition temperature of both. Also, because of the very low electrical conductivity of SU-8 fibers, the high voltages applied during electrospinning exert an extra mechanical force on the polymer nanofibers during their formation, stretching and disentangling the polymer chains. Moreover, carbonization of one-dimensional, suspended polymer structures, with all surfaces exposed during pyrolysis, is bound to give a different morphology than surface attached structures. Finally, making the wires shorter gives one a higher probability of obtaining CNWs that contain continuous graphite sheets without defects or bending of graphitic planes from contact to contact (explained in detail with HR-TEM pictures, Figure 3). Figure 3A–D illustrates four different types of CNWs that can be observed in the same batch of fibers. Most CNWs have core–shell geometry. However, the thickness of graphitic shell may slightly vary because the distribution of polymer chains may not be uniform at nanoscale in the polymer solution itself. Images E and F in Figure 3 display HR-TEM images of pure graphite and glassy carbon, and it can be clearly observed that carbon chains form loops in polymer derived glassy carbons and it is almost impossible to disentangle them after carbonization.

These parameters are not necessarily independent; nor are their relative importance in enhancing the graphitic content of the wires known. Our group has started to address the relative influence of these different parameters on the extent of graphitization. In a previous work, we discussed the results of conductivity measurements on single suspended CNWs derived from two different polymers (parameter 1).[24] The carbon fibers studied were only moderately stretched with diameters ~200 nm (parameter 6), and no additional mechanical stretching (parameter 5) was employed during fabrication. The relatively large diameters also did not allow elucidation of nanoconfinement or surface effects.

In the current paper we emphasize fabrication of structures for use in evaluating the influence of parameters 4, 5, and 6 and the additional plausible parameters listed above by monitoring the change in resistance and structural changes in the fabricated CNWs. Besides impedance measurements, high-resolution transmission electron microscopy (HR-TEM), Raman spectroscopy, X-ray diffraction (XRD), and scanning electron microscopy (SEM) were carried out to correlate nanowire structure with resistance data.

A typical MEMS structure featuring SU-8 walls that was used to anchor electrospun suspended nanowires is schematically shown in Figure 1A. In this design, two SU-8 contact pads (5.0 mm × 5.0 mm) are connected to two SU-8 walls 20 μm wide with a 20 μm gap in between. The SU-8 posts are about 10 μm high, which shrink to ~2 μm height after pyrolysis. In Figure 1B, we schematically illustrate photoelectrospinning of SU-8 on an SU-8 MEMS structure employing a rotating drum collector, whereas in Figure 1C we display a Si chip (2 cm × 1 cm) patterned with a CNW-CMEMS structure that is obtained by the pyrolysis of the polymer precursor structures. The rotating drum forces the fibers to follow a straight pattern that we orient perpendicularly to the electrodes, and because of the drum's rotation, the fibers remain taut without touching the substrate.

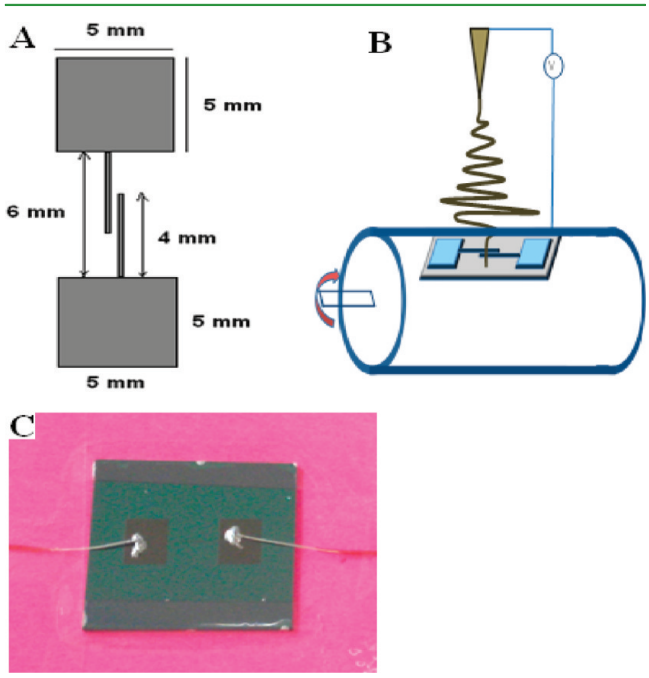

Figure 1. (A) 2D representation of SU-8 MEMS structure used as base structure for electrospinning nanofibers. Both thickness and the gap between two stripes are 20 μm. (B) Use of rotating drum as collector for electrospinning SU-8 nanofibers on SU-8 MEMS chip. (C) Final chip-based CMEMS-CNW design on a Si chip fabricated as described in A and B and pyrolyzed at 900 °C (electrical connections were made only after pyrolysis).

Flow and electrical field are both expected to facilitate molecular disentanglement (parameters 4 and 5). And as we also speculate here the rotating drum introduces a considerable additional mechanical pull on the nanowires that may further enhance graphitization by molecular combing (parameter 6).

In case more than one carbon nanofiber linked the walls, the extra fibers were cut using a gallium ion beam dual focused ion beam (FIB) system. The MEMS design employed in our fabrication has 2 mm long overlapping electrodes. The number of fibers linking these electrodes can be controlled by reducing the time of electrospinning and the overlapping area of the electrodes. In this study we perform electrospinning for 3–5 seconds, which yields a single CNW in most cases. However, if two fibers fallen at the same time connect the electrodes, the undesired extra fiber can be cut using FIB.

The FIB wire cutting is illustrated in Figure 2A. After confirming that only one suspended carbon wire remained, the

dx.doi.org/10.1021/am2014376 | ACS Appl. Mater. Interfaces 2012, 4, 34–39

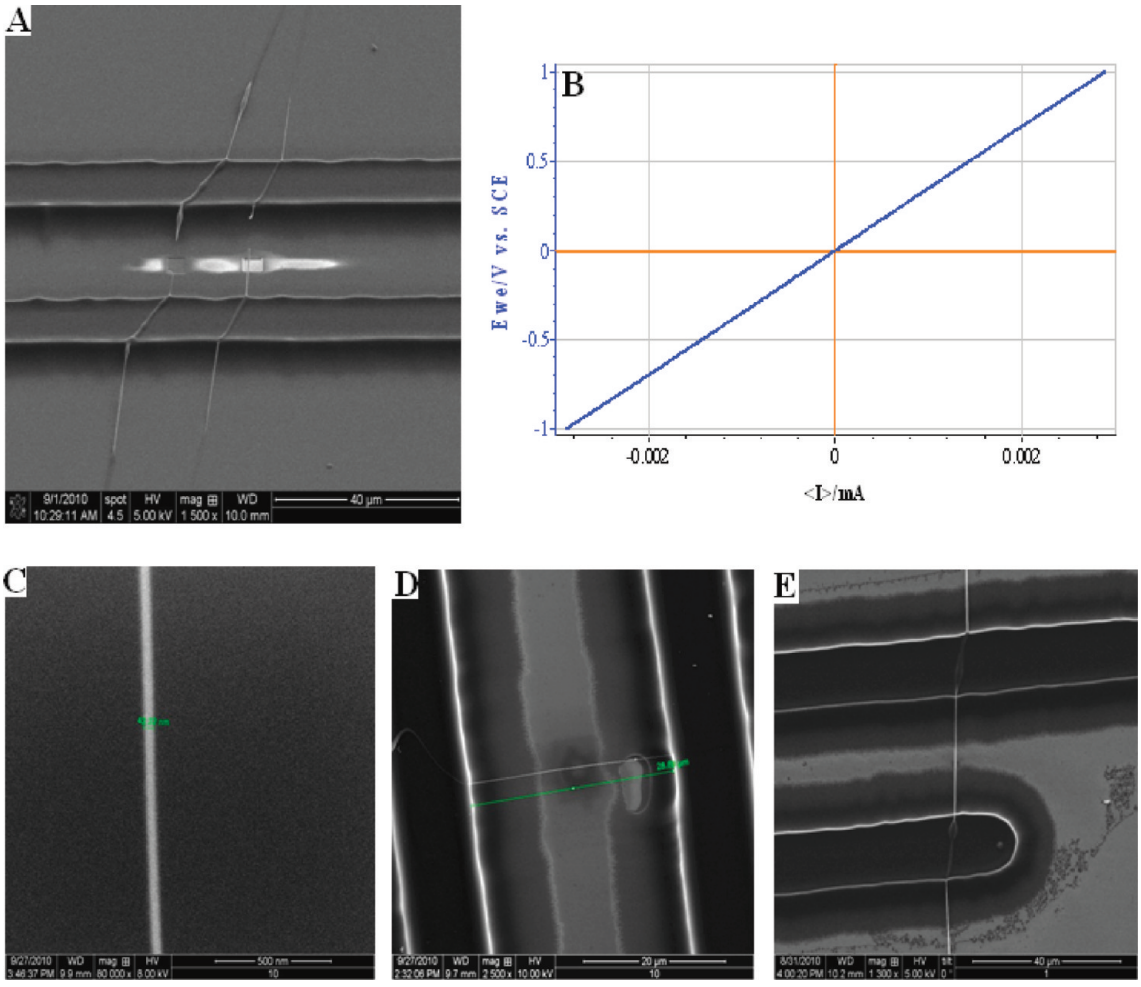

Figure 2. (A) FIB cutting for extra CNWs. (B) Typical $I-V$ curve for a single suspended CNW. (C, D) SEM images displaying (C) the diameter and (D) length of a single suspended CNW. (E) Low-magnification SEM image displaying the adhesion of CNW on to CMEMS electrode walls.

carbon electrode pads were connected to Cu wires with silver paste that then were connected to an impedance analyzer (Figure 1C). Figure 2B shows a typical $I-V$ curve for a 42.2 nm thick and ~29 μm long single suspended CNW obtained using the impedance analyzer connected to the measuring chip (illustrated in Figure 1C). The structures of these CNWs were further characterized with SEM, Raman spectroscopy, XRD, and HR-TEM imaging.

Typical SEM images of single suspended CNWs are shown in Figure 2C–E. In Figure 2C, D, a 42.22 nm thick nanowire with a length of ~29 μm is shown. It can be observed in Figure 3D that the CNWs have a very uniform geometry. However, to account for any experimental or imaging error in determining the diameter of CNWs, we took SEM pictures at 3–4 different points along the length of the wire. Uniformity of the wires to within 10% was observed. In Figure 2E, a lower-magnification SEM image illustrates the adhesion of a typical CNW onto the carbon walls. As the SU-8 MEMS structure and suspended SU-8 nanowire are pyrolyzed together, this technique yields CNWs with very good adhesion to the walls. Also, the electrical measurements confirm that an ohmic contact between wire and walls is realized automatically without the need for any other contacting metal or further sintering.

The linearity of all $I-V$ curves thus obtained is evidence for the ohmicity of the carbon-to-carbon contacts. In Table 1 we compare the electrical conductivity values of five different diameter wires as obtained from the slope of $I-V$ curves. While calculating the conductivity values, length, and diameters of CNWs were accounted for. We observe that for the CNWs in diameter range 42–113, the conductivity is a materials property and thus remains constant.

The average value for the electrical conductivity of the CNWs was found to be 6.13×10^4, which is almost twice that of glassy carbon (2.8×10^4).[33] The reported electrical conductivity values for graphite range from 2.4×10^4 to 1.02×10^5 observed parallel and perpendicular to the C-axis, respectively.[34] Our experimental conductivity values are lower than graphite but higher than glassy carbon. These results indicated that electrospun SU-8 derived CNWs fabricated with additional mechanical pulling are not composed entirely of glassy carbon. On the basis of previous CMEMS work[2] with carbonization of SU-8, one expects that the resulting carbon would be completely glassy in nature and that the suspended carbon wires would shrink by approximately 80–90% of the original polymer wire diameter. However, these wires shrunk only by approximately 30% of the original wire diameter as confirmed by SEM images. These unexpected observations on electrical conductivity and shrinkage during pyrolysis led us to investigate the structure and composition of the CNWs. An earlier study[24] reported a lower value for the SU-8 derived carbon wires of ~200 nm diameter, which was most likely due to their higher contact resistance as they could not be spun and

dx.doi.org/10.1021/am2014376 | ACS Appl. Mater. Interfaces 2012, 4, 34–39

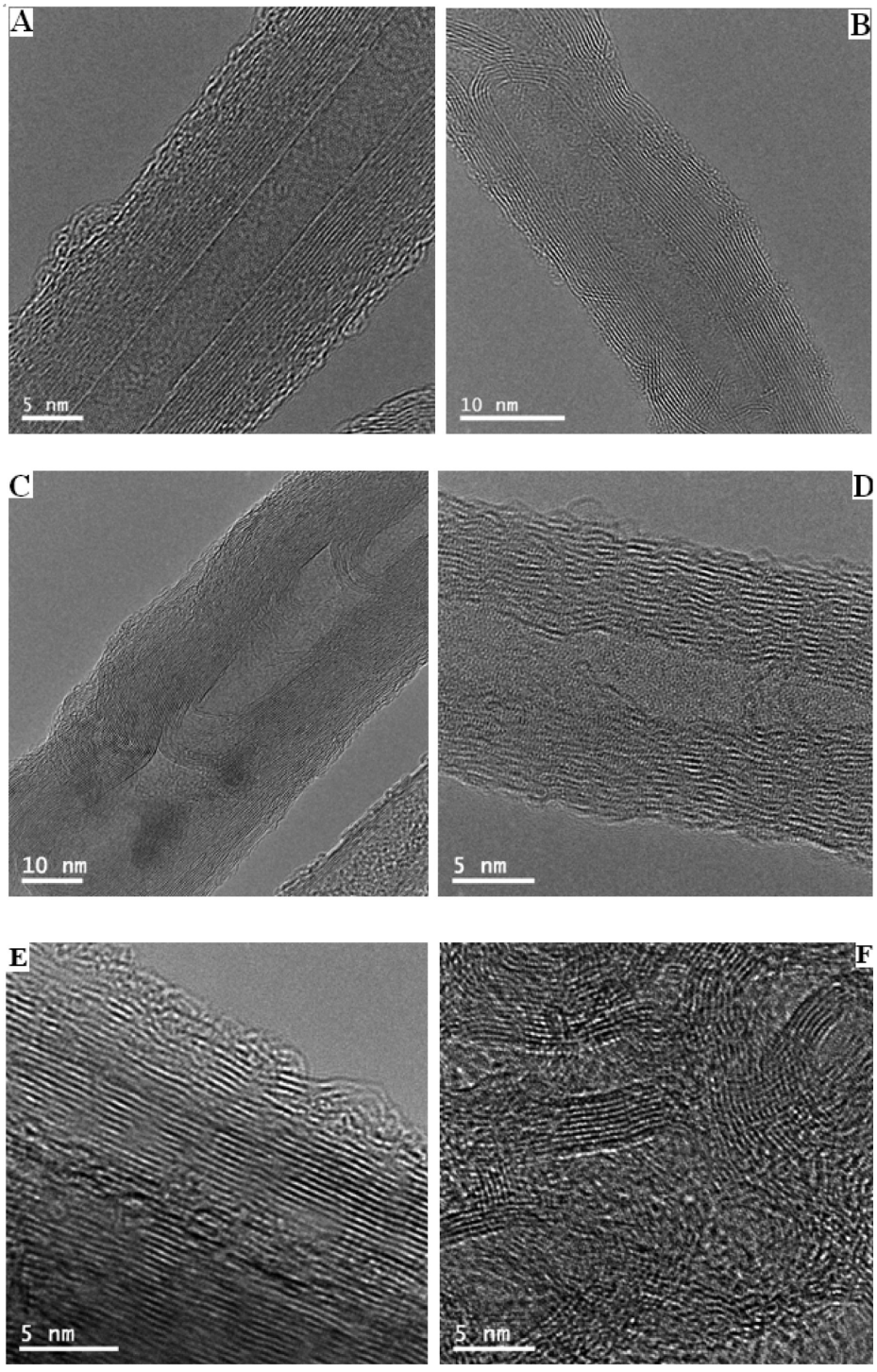

Figure 3. (A–D) HR-TEM images of SU-8 derived CNWs: (A) Tubelike graphitic CNW with glassy carbon core and graphite shell. (B) Glassy carbon trapped between graphitic walls in a CNW. (C) Graphite layers bending inward at various segments of a CNW. (D) Tubelike graphitic CNW with graphite shell not well-formed. (E) Pure graphite obtained from pencil flakes. (F) Pure glassy carbon obtained from a pyrolyzed thick SU-8 structure.

Table 1. Comparison of the Conductivity of SU-8 Derived Single Suspended CNWs of Different Diameters

diameter of nanowire (nm)	observed value of conductivity (S/m)
42.22	$6.16\ (\pm 0.23) \times 10^4$
71.16	$6.96\ (\pm 0.17) \times 10^4$
107.0	$5.33\ (\pm 0.21) \times 10^4$
113.0	$6.07\ (\pm 0.19) \times 10^4$

integrated tightly on to the posts without mechanical action of pulling on a rotating drum as used here.

The HR-TEM images in Figure 3A–D indicate formation of ordered surface domains with a more disordered glassy core. The presence of a graphitic skin layer could explain the higher conductivity and a lack of greater shrinkage associated with the production of glassy carbon. Such structures support the theoretical model of polymer chain orientation suggested by Ji

dx.doi.org/10.1021/am2014376 | ACS Appl. Mater. Interfaces 2012, 4, 34–39

et al.[25] With repeated HR-TEM experiments, we also observed bending of graphitic planes (Figure 3C), something that should also influence the conductivity.[35]

Figure 4A displays the Raman spectra for SU-8 derived CNWs. The fraction of disordered carbon in these wires

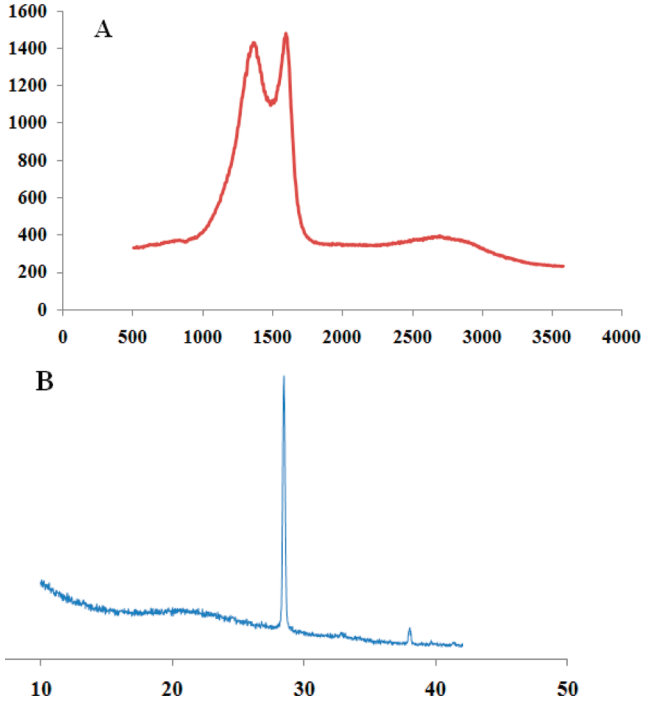

Figure 4. (A) Raman spectra of SU-8 derived CNWs. (B) XRD data for SU-8 derived CNWs (Y axis, intensity in a.u.; X axis, 2θ in deg).

(calculated as the area fraction of the first peak, I_d)[36] is lower than the fraction of graphitic carbon (area fraction of the second peak, I_g); however, we can observe the presence of both amorphous and crystalline carbon. The fraction of graphite in the resulting carbon is 0.61 which indicates that a slightly higher amount of graphitic carbon than amorphous is present in the wires.

The results of XRD are represented in Figure 4B. We can clearly observe the characteristic sharp peak for graphite at 2θ value 28.[37] The diffused peaks appearing at 2θ values 10−23 confirm the presence of amorphous or glassy carbon with some degree of crystallinity.[38] These results again confirm the partially graphitic nature of CNWs.

According to Harris,[22] carbons obtained from the pyrolysis of polymers contain six, five and seven membered rings, the latter two cause the bending of graphitic planes. This bending effect can be observed in our HR-TEM pictures (Figure 3C). It appears that the stretching action of the combined mechanical and electrostatic forces during electrospinning on a drum greatly reduces the polymer chain entanglement leading to their alignment and to more graphitic CNWs. SU-8 has very low electrical conductivity and therefore very high voltages are applied during electrospinning. The charged SU-8 fibers are pulled from both ends by electrical force and this leads to better electrical combing leading to chain disentanglements. In contrast, carbonization of the underlying photolitographically defined SU-8 (as in the contacting walls) continues to yield completely glassy carbon as expected. This supports the idea that the enhanced graphitization of SU-8 derived CNWs is affected by the fabrication technique used. The improved graphitization of the CNWs fabricated here by electrospinning is thus engendered by one or more of the following factors: (1) flow of the polymer/solvent jet with a diameter similar to that of the gyration radius of the constituent polymer molecules,[25] (2) mechanical pulling of fibers during the electrospinning on a drum, (3) high electrical forces employed in electrospinning acting on the charged SU-8 polymer (electrical molecule combing) and, (4) pyrolysis of a free-standing one- dimensional structure instead of an anchored three-dimensional large polymer structure.

In summary, we have demonstrated a method for the fabrication of sub-50 nm diameter suspended carbon wires of predefined length and position by controlled electrospinning. These wires are monolithically integrated with an underlying CMEMS structure. The method is compatible with standard photolithography and electrospinning techniques and materials (SU-8 photoresist) allowing for easy integration with mass manufacturing. The most important advantage of our fabrication methodology is that we obtain a monolithic device with no glue or clips required to hold the nanowire in place. This technique is a very simple and inexpensive way for fabricating carbon nanowires with very high aspect ratios. Also, no effort is required for isolation and positioning of a single CNW from a collection of wires. The wires are free-standing and they are pulled in tension due to the mechanical stretching caused by the rotating drum. The stretching of the polymer chains and surface confinement in these CNWs produce a graphitic skin and an amorphous core, thus enhancing the CNW electrical conductivity compared to pure glassy carbon. We also analyzed all the parameters that may improve chain disentanglements in polymer nanofibers that subsequently lead to more graphitic CNWs. A complete understanding and control over these parameters will enable the production of all graphite nanowires from contact to contact, i.e., nanocables that exhibit a band gap equivalent to de Heer et al.'s graphene ribbons.[39]

EXPERIMENTAL SECTION

High-resistivity Si wafers (25−40 kΩ) coated with an 800 nm thick layer of thermal SiO_2 were utilized as substrates to ensure a completely insulated surface for electrical characterization of the carbonized fibers and CMEMS structure. Epoxy-based negative photoresist, SU-8 2010 (2000 series cyclopentanone-based formulation obtained from Micro Chem, MA) without any additional solvents was electrospun to produce SU-8 nanofibers on the SU-8 walls. We employed standard photolithography to fabricate the SU-8 MEMS contact structures that predefine the length of the electrospun SU-8 fibers.[2,24] Electrospinning was carried out on a electrospinner (NF Series, MECC, Japan) with a rotating drum collector. The rotating drum collector's speed during electrospinning was 2000 rpm and MEMS chips were fixed onto the drum with scotch tape. The flow rate of the SU-8 photoresist was 1 mL/h throughout the short 3−5 s electrospinning process. The distance between the polymer jet's point of initiation and the rotating collector was 10 cm. The applied voltage was 22−24 kV. In 3−5 s of electrospinning, we typically obtained between 1 to 5 nanofibers suspended between the SU-8 walls. The fibers were exposed to UV light to initiate cross-linking. Pyrolysis of these SU-8 nanofibers and SU-8 walls was carried out at 900 °C for 1 h in a vacuum furnace (R. D. WEBB 2704, USA); the temperature ramp up was 1 °C/min.

dx.doi.org/10.1021/am2014376 | ACS Appl. Mater. Interfaces 2012, 4, 34−39

Impedance measurements on the suspended single CNWs ranging from 42.2- 113.0 nm in diameter were carried out using a VSP impedance analyzer (BioLogic, S.Korea). For HR-TEM, Raman spectra, and X- ray diffraction, the samples were prepared as nanowire mats rather than individual fibers. An average value of graphitization of nanowires in the laser/X-ray beam was calculated. HR-TEM imaging was carried out on a JEM-2100F (Cs) machine (JEOL, Japan), Raman spectra and X- Ray Diffraction patters were obtained on a WITec alpha300R Micro Raman instrument (532 nm) and X' Pert PRO, (PANanalytical, Netherlands) using Cu Kα radiation respectively. SEM and FIB imaging were carried out on a dual beam FIB system (Quanta 3D FEG, FEI, USA).

There is a major difference in the fabrication method employed here compared to our earlier work.[24] Earlier, electrospinning was done on electrically conducting posts without a rotating drum.[24] The electrospun nanofibers did not connect to the posts if the posts were not conducting. In the present technique, nanowire connections can be formed directly on nonconducting SU-8 walls by mechanical means, i.e., action of the rotating collector. The whole structure (underlying SU-8 MEMS platform plus wires) is pyrolyzed after the formation of nanowires. The earlier technique[24] is thus more suitable for the formation of large area networks in which an array of microposts are to be connected by self-assembly engendered by electrically conducting posts. The current technique, however, appears to be more attractive for a tighter integration of the nanowires with the underlying microstructure and thus for a more accurate testing of the electrical properties of single wires.

AUTHOR INFORMATION

Corresponding Author

*E-mail: mmadou@uci.edu (M.M.); ashutos@iitk.ac.in (A.S.). Tel.: +1-9499815672 (M. M.); +91 512 2597026 (A.S.).

ACKNOWLEDGMENTS

This work was supported by World Class University (WCU) program *R*32-2008-000-20054-0 at UNIST, South Korea; UC Lab Fees Award 09-LR-09-117362 at UC, Irvine, CA, USA, and the Unit on Soft Nanofabrication and IRHPA research grants from the Department of Science and Technology, New Delhi at IIT, Kanpur, India. A.S. and M.M. also acknowledge support from the Indo-US Science and Technology Forum, New Delhi.

REFERENCES

(1) Kinoshita, K. *Carbon: Electrochemical and Physicochemical Properties*; Wiley: New York, 1988.

(2) Wang, C.; Zaouk, R.; Park, B. Y.; Madou, M. J. *J. Manuf. Technol. Manage.* **2008**, *13*, 360−375.

(3) Gates, B. D.; Xu, Q.; Stewart, M.; Ryan, D.; Willson, C. G.; Whitesides, G. M. *Chem. Rev.* **2005**, *105*, 1171−1196.

(4) Madou, M. J. *Fundamentals of Microfabrication*, 1st ed.; CRC Press: Boca Raton, FL, 1997.

(5) McCreery, R. *Special Issue: Molecular Electronics Interface (The Electrochem. Soc.)* **2004**, *13* (1), 46−51.

(6) Schueller, O. J. A.; Brittain, S. T.; Whitesides, G. M. *Adv. Mater.* **1997**, *9*, 477−480.

(7) Baughman, R. H.; Zakhidov, A. A.; DeHeer, W. A. *Science* **2002**, *297*, 787−792.

(8) McCreery, R. L. *Chem. Rev.* **2008**, *108*, 2646−2687.

(9) Dresselhaus, M. S.; Dresselhaus, G.; Avouris, Ph., Eds. *Carbon Nanotubes*; Springer: New York, 2001.

(10) Chen, P.; McCreery, R. L. *Anal. Chem.* **1996**, *68*, 3958−3965.

(11) Marsh, H.; Heintz, E. A.; Rodrigues-Peinoso, F., Eds. *Introduction to Carbon Technologies*; University of Alicante: San Vicente del Raspeig, Spain, 1997.

(12) Kinoshita, K. *New Trends in Electrochemical Technology, Vol. 1: Energy Storage Systems for Electronics*; Osaka, T., Datta, M., Eds.; Gordon and Breach, Reading, U.K., 1999; p 193.

(13) Bosnick, K.; Gabor, N.; McEuen, P. L. *Appl. Phys. Lett.* **2006**, *89* (163121), 1−3.

(14) Ilani, S.; Donev, L. A. K.; Kindermann, M.; McEuen, P. L. *Nat. Phys.* **2006**, *2*, 687−691.

(15) Sazonova, V.; Yaish, Y.; Ustunel, H.; Roundy, D.; Arias, T. A.; McEuen, P. L. *Nature* **2004**, *431*, 284−287.

(16) DeVolder, M. F. L.; Vansweevelt, R.; Wagner, P.; Reynaerts, D.; Van Hoof, C.; Hart, A. J. *ACS Nano* **2011**, *5* (8), 6593−6600.

(17) Chen, W.; Beidaghi, M.; Penmatsa, V.; Bechtold, K.; Kumari, L.; Li, W. Z.; Wang, C. *IEEE Trans. Nanotechnol.* **2010**, *9* (6), 734−740.

(18) Chai, Y.; Wu, Y.; Takei, K.; Chen, H. Y.; Yu, S.; Chan, P. C. H.; Javey, A.; Wong, H. S. P. *2010 IEEE International Electron Devices Meeting (IEDM)*; San Francisco, Dec 6−8, 2010 ; IEEE: Piscataway, NJ, 2010; pp 214−217.

(19) Huang, J; Wan, Q. *Sensors* **2009**, *9*, 9903−9924.

(20) Bibekananda, S.; Babu, V. J.; Subramanian, V.; Natarajan, T. S. *J. Eng. Fibers Fabr.* **2008**, *3* (4), 39−45.

(21) Jenkins, G. M.; Kawamura, K. *Nature* **1971**, *231*, 175−176.

(22) Harris, P. J. F. *Philos. Mag.* **2004**, *84* (29), 3159−3167.

(23) Franklin, R. E. *Proc. R. Soc. London, Ser. A* **1951**, *209*, 196−218.

(24) Sharma, C. S.; Katepalli, H.; Sharma, A.; Madou, M. J. *Carbon* **2011**, *49*, 1727−1732.

(25) Ji, Y.; Li, C.; Wang, G.; Koo, J.; Ge, S.; Li, B.; Jiang, J.; Herzberg, B.; Klein, T.; Chen, S.; et al. *EPL* **2008**, *84* (56002), 1−6.

(26) Ehrenstein, G. W.; Theriault, R. P. *Polymeric Materials: Structure, Properties, Applications*; Carl Hanser Verlag: Munich, Germany, ; p 67.

(27) Ko, F.; Gogotsi, Y.; Ali, A.; Naguib, N.; Ye, H.; Li, C.; Willis, P. *Adv. Mater.* **2003**, *15* (14), 1161−1165.

(28) Lozano, K.; Sarkar, K. U.S. Patent 0 280 325 A1 2009.

(29) Kim, J. M.; Ohtani, T.; Park, J. Y.; Chang, S. M.; Muramatsu, H. *Ultramicroscopy* **2002**, *91* (1−4), 139−149.

(30) Oya, A.; Marsh, H. *J. Mater. Sci.* **1982**, *17*, 309−322.

(31) Du, R.; Ssenyange, S.; Aktary, M.; McDermott, M. T. *Small* **2009**, *5* (10), 1162−1168.

(32) Sevilla, M.; Fuertes, A. B. *Carbon* **2006**, *44*, 468−474.

(33) Serway, R. A.; Faughn, J. S. *College Physics*, 6th ed.; Thomson: Belmont, CA, 2003.

(34) Powell, R. L.; Childs, G. E. *American Institute of Physics Handbook*; McGraw-Hill, New York, 1972; pp 4−142.

(35) Dutta, A. K. *Phys. Rev.* **1953**, *90* (2), 187−192.

(36) Ra, E. J.; An, K. H.; Kim, K. K.; Jeong, S. Y.; Lee, Y. H. *Chem. Phys. Lett.* **2005**, *413* (1−3), 188−193.

(37) Saenger, K. L.; Tsang, J. C.; Bol, A. A.; Chu, J. O.; Grill, A.; Lavoie, C. *Appl. Phy. Lett.* **2010**, *96* (153105), 1−3.

(38) Hussain, R.; Qadeer, R.; Ahmad, M.; Saleem, M. *Turk. J. Chem.* **2000**, *24*, 177−183.

(39) DeHeer, W. A.; Berger, C.; First, P. N. U.S. Patent 7 015 142, 2006.